G. Pagliarini
Associate Professor,
Istituto di Fisica Tecnica,
Università degli Studi di Bologna,
40136 Bologna, Italy

G. S. Barozzi
Full Professor,
Istituto di Fisica Tecnica,
Università degli Studi di Trieste,
34127 Trieste, Italy

Thermal Coupling in Laminar Flow Double-Pipe Heat Exchangers

Thermal interaction between the streams of laminar flow double-pipe heat exchangers is investigated theoretically by accounting for axial conduction along the wall separating the fluids. In a countercurrent arrangement, thermal coupling is demonstrated to have a definite influence on all the more important heat transfer parameters, such as the wall temperature, the heat flux density, the local entropy production rate, and the Nusselt number distributions. The overall performance of the device is considered under a second law point of view, and a complete parametric study is carried out.

1 Introduction

Parallel plate and double pipe heat exchangers find current application in industrial processes for energy conversion. The need for accurate sizing of the equipment and its thermodynamic optimization increases when the temperature difference between the fluids decreases and becomes paramount when a very high efficiency is demanded.

A basic unit essentially consists of two flow passages separated by a conducting wall. Through this, the two heat carriers thermally interact, flowing either concurrently or countercurrently. A double-pipe device can therefore be schematized into a couple of concentric tubes, the inner one providing the heat transfer surfaces.

As discussed in classical thermal engineering textbooks (Kays and London, 1984; Kakac et al., 1981; Spalding, 1984), two essential assumptions are customarily made in the design of heat exchangers: (*i*) The film coefficients are considered to be insensitive to the longitudinal distribution of both the heat flux and the surface temperature; and (*ii*) they are taken to be uniform, irrespective of the heat exchanger length. There is substantial evidence (Stein, 1966a) that based upon the above assumptions, the sizing of the heat transfer surfaces is satisfactory for turbulent flow conditions. The local heat transfer rate is scarcely influenced by the thermal boundary conditions in those cases, and the thermal inlet region usually covers a small part of the heat transfer length. When dealing with laminar flow conditions, however the thermal inlet length can often be of the same order of magnitude as the heat exchanger length. Film coefficients are by no means uniform and also become very sensitive to the thermal boundary condition. Since the two streams are thermally coupled by the conducting wall, the boundary condition for each of them is not defined a priori. It is instead dependent on the geometry and the thermal properties of the wall, other than the operating conditions of the device. The problem is made even more complex when axial conduction along the wall is taken into account. Axial wall conduction affects both the distributions of the heat transfer coefficients and the overall thermal performance of the device.

In this paper, the effects of thermal coupling in double-pipe heat exchangers are dealt with. Heat conduction along the wall is accounted for in the analysis and its influence on heat exchanger effectiveness and entropy production is discussed.

2 Literature Survey

The earliest investigations on double current laminar heat exchangers are due to Stein (1964, 1965a, 1965b) who presented an analytical solution for concurrent flow. The mathematical aspects associated with countercurrent flow were first discussed by Nunge and Gill (1965). They also presented extensive results for double-pipe heat exchangers (Nunge and Gill, 1966). The approach was based upon the reduction of the primitive double-region problem into a couple of one-region Sturm–Liouville problems. Coupling conditions had to be matched at the common boundary, and an equivalent of the orthogonality condition devised over both regions. This constitutes a major difficulty in orthogonal expansion solutions and the accuracy of the procedure used by Nunge and Gill has actually been questioned (see Stein, 1966b, and Blanco et al., 1968, for discussion). Stein (1966a, 1966c) presented a generalization of the method for both concurrent and countercurrent flow. The method was extended by Blanco and Gill (1967) to the case of slug flow rather than fully developed laminar flow, while the effects of axial conduction in the fluids were considered by Nunge et al. (1967). The superposition of known solutions in the form of the Duhamel theorem was applied to the concurrent case by Gill et al. (1968). An alternative approach is based on the expression of the temperature field in each stream in terms of unknown functions of the heat flux across the walls, thus creating a system of cross-linked integral equations to be solved numerically. This was adopted by Bentwich (1970, 1973) to deal with two-stream and multistream parallel-flow heat exchangers. An original general methodology for conjugated problems was presented by Papoutsakis and Ramkrishna (1981). The energy equation was decomposed into a system of first-order differential equations, which again gave a Sturm–Liouville problem. Sample temperature distributions in concurrent and countercurrent heat exchangers were presented on account of axial heat conduction in the two streams. An efficient algorithm for solving two Sturm–Liouville equations coupled at a common boundary was given by Mikhailov (1972, 1973a). The analytical solution was based upon a finite integral transform and applies to a wide class of conjugated boundary value problems. A specialized version of the method for conjugated Graetz problems was formulated by Mikhailov (1973b, 1983) and illustrative examples were presented by Mikhailov and Shishedjiev (1976), among which the case of concurrent double pipe heat exchanger was treated. The same problem has recently been treated by Cotta and Ozisik (1986) using a more refined version of the same method. Finally, a fully numerical solution for developing flow in countercurrent double-pipe heat exchangers has been presented by Lin and Tsay (1986).

Under the assumptions of fully developed laminar flow and constant property fluids, a few general comments can be made on the thermal behavior of double-stream heat exchangers.

With concurrent flow:

(*i*) A thermally developed region always exists asymptotically. This may or may not be attained in practical cases, depending on the heat exchanger length. The length of the

Contributed by the Heat Transfer Division for publication in the JOURNAL OF HEAT TRANSFER. Manuscript received by the Heat Transfer Division July 5, 1989; revision received November 9, 1990. Keywords: Conjugate Heat Transfer, Heat Exchangers, Thermodynamics and Second Law.

thermal inlet region is a function of the wall thermal resistance, fluid properties and the operating conditions.

(*ii*) Asymptotic values of the heat transfer coefficient can be significantly less than those corresponding to the boundary condition of uniform wall temperature, condition (T), for single-stream cases. They cannot be larger than values corresponding to the boundary condition of uniform heat flux, condition (H) (Stein, 1965a). Such behavior is consistent with single-stream heat transfer results when imposing an exponentially decreasing heat flux at the duct wall (Shah and London, 1978).

(*iii*) Distributions of the heat transfer coefficient in the thermal inlet region show good agreement with single-stream solutions for case (T). Despite this, the wall temperature can exhibit significant longitudinal variations (Gill et al., 1968).

With countercurrent flow:

(*i*) The heat transfer rate decreases monotonically from the extremities to the central part of the heat transfer length where a minimum is always achieved. Eventually, a central region of thermally developed flow can occur, according to the heat exchanger geometry and the operating conditions.

(*ii*) Asymptotic values of the heat transfer coefficients are never less than values corresponding to case (T), but can be significantly larger than reference values for the boundary condition (H) (Stein, 1966a).

(*iii*) For each stream, the heat transfer coefficient is bounded by single-stream solutions (T) and (H) close to the entrance (Lin and Tsay, 1986). It may be worth noting that in spite of the influence of thermal coupling on the distributions of film coefficients an overall heat transfer coefficient can still be defined. According to the Seban et al. (1972) approximate method, this can be used with sufficient accuracy.

(*iv*) The effect of axial heat conduction in fluids is generally negligible for Peclet numbers greater than 100 (Nunge et al., 1967).

In all the above literature, the effect of axial conduction along the wall separating the two streams was overlooked. This has been recognized to have a definite effect on heat transfer

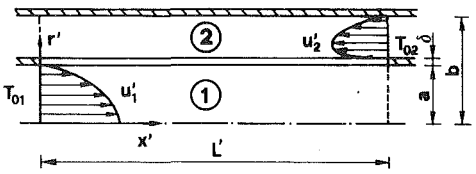

Fig. 1 Schematic of the double-pipe heat exchanger

efficiency in countercurrent flow (Kroeger, 1966; Barron and Yeh, 1976) and crossflow (Chiou, 1983) heat exchangers. Very accurate results for the laminar flow case were given by Mori et al. (1980) for parallel plate countercurrent heat exchangers. Sample data for both concurrent and countercurrent double pipe heat exchangers were presented by the authors (1984a).

Double-stream heat exchangers have also been extensively investigated from a thermodynamic point of view, and many valuable second law analyses can be mentioned (see, for example, Bejan, 1977; Golem and Brzustowski, 1976; Ciampi and Tuoni, 1979). In all of them, however, the lumped system approach has been employed, while assuming a uniform heat transfer coefficient and omitting axial wall conduction. The latter effect was considered by Chowdhury and Sarangi (1983), who also derived a simple formula to optimize the thermal conductivity of the wall. That criterion has been found to be valid even in the case of laminar balanced counterflow heat exchangers (Pagliarini and Barozzi, 1984b, 1985).

3 Analysis

The system under consideration is schematically depicted in Fig. 1. Two Newtonian constant property fluids are assumed to flow under steady and laminar conditions through the equipment with fully developed velocity profiles. Internal heat generation, viscous dissipation, and axial heat conduction in the fluids are neglected.

According to the notation in the figure, indexes 1 and 2, respectively, designate the inner and outer stream. It is assumed that heat is transferred from stream 2 to stream 1. The fluid

Nomenclature

a = internal radius of the inner duct (Fig. 1)
b = internal radius of the outer wall of the outer duct (Fig. 1)
B = radius ratio $= b/a$
c_p = specific heat at constant pressure
d_h = hydraulic diameter
H = ratio between the flow-stream capacity rate of outer and inner flow $= (m\ c_p)_2/(m\ c_p)_1$
(H) = thermal boundary condition referring to uniform wall heat flux
k = thermal conductivity
K = nondimensional thermal conductivity $= k/k_1$
K_{opt} = optimum K value $= \mathrm{Pe}_1/[2(1+H^{-1})]$, from Chowdhury and Sarangi (1983, equation (11))
L' = dimensional length of the heat exchanger
L = nondimensional length of the heat exchanger $= L'/a$
L^* = nondimensional length of the heat exchanger $= L'/(2\ a\ \mathrm{Pe}_1)$
m = mass flow rate
Nu = Nusselt number (equations (8))
Pe = Peclet number $= U\ d_h\ (c_p\ \rho/k)_f$
q = nondimensional heat flux at the solid-fluid interface (equations (6))
Q = heat transferred per unit time from stream 2 to stream 1
r' = dimensional radial coordinate
r = nondimensional radial coordinate $= r'/a$
s = rate of entropy production per unit volume
S = rate of entropy production
T = absolute temperature
T_0 = absolute inlet temperature
(T) = thermal boundary condition referring to uniform wall temperature
u' = dimensional axial velocity
u = nondimensional axial velocity $= u'/U$
U = fluid mean axial velocity
x' = dimensional axial coordinate
x^* = nondimensional axial coordinate $= x'/(2\ a\ \mathrm{Pe}_1)$
z^* = nondimensional axial coordinate $= L^* - x^*$
Γ = nondimensional inlet temperature of the outer stream $= T_{02}/T_{01}$
δ = wall thickness
Δ = nondimensional wall thickness $= (\delta/a)$
ϵ = heat exchanger effectiveness (equation (14))
Θ = nondimensional temperature $= T/T_{01}$
Θ_b = nondimensional bulk fluid temperature (equation (7))
Θ_w = nondimensional temperature at the wall-fluid interface
ρ = density
σ = nondimensional rate of entropy production per unit volume (equation (9))
Σ = nondimensional rate of entropy production

Subscripts

f = fluid
s = solid
x = local value
w = wall-fluid interface
1 = inner stream
2 = outer stream

temperature is uniform at the inlet sections; the condition $T_{02} > T_{01}$ therefore holds.

For the sake of brevity, the mathematical problem is directly stated in nondimensional terms. Use is made of symbols and definitions given in the Nomenclature. The system is subdivided into three physically homogeneous regions, namely, stream 1, stream 2, and the solid wall separating the fluids.

For each region the energy equation is written:

Stream 1:

$$u_1 \frac{\partial \Theta_1}{\partial x^*} = 4\left(\frac{1}{r}\frac{\partial \Theta_1}{\partial r} + \frac{\partial^2 \Theta_1}{\partial r^2}\right) \qquad 0 \le x^* \le L^*, \quad 0 \le r \le 1 \tag{1}$$

$$\Theta_1(0, r) = \Theta_{01} \tag{1a}$$

$$\frac{\partial \Theta_1}{\partial r}(x^*, 0) = 0 \tag{1b}$$

Solid Wall:

$$4\,\mathrm{Pe}_1^2\left(\frac{1}{r}\frac{\partial \Theta_s}{\partial r} + \frac{\partial^2 \Theta_s}{\partial r^2}\right) + \frac{\partial^2 \Theta_s}{\partial x^{*2}} = 0 \quad 0 \le x^* \le L^*, \quad 1 \le r \le 1+\Delta \tag{2}$$

$$\frac{\partial \Theta_s}{\partial x^*}(0, r) = \frac{\partial \Theta_s}{\partial x^*}(L^*, r) = 0 \tag{2a}$$

Stream 2:

$$u_2 \frac{\partial \Theta_2}{\partial x^*} = 4\,\frac{K_f}{H}\,(B^2 - (1+\Delta)^2)\left(\frac{1}{r}\frac{\partial \Theta_2}{\partial r} + \frac{\partial^2 \Theta_2}{\partial r^2}\right) \qquad 0 \le x^* \le L, \quad 1+\Delta \le r \le B \tag{3}$$

$$\Theta_2(0, r) = \Theta_{02} \quad \text{(concurrent case)}$$
$$\Theta_2(L^*, r) = \Theta_{02} \quad \text{(countercurrent case)} \tag{3a}$$

$$\frac{\partial \Theta_2}{\partial r}(x^*, B) = 0 \tag{3b}$$

In equations (1) and (3), u_1 and u_2 are nondimensional distributions of the fluid velocity, as given in the literature (e.g., Shah and London, 1987, Chap. 5, p. 78, and Chap. 12, p. 205, for circular and annular ducts, respectively). Pe_1 is the Peclet number for the inner stream, H is the thermal capacity ratio of the streams, $H = (mc_p)_2/(mc_p)_1$, and Δ is the nondimensional wall thickness.

Continuity conditions for the temperature and the heat flux apply at the interfaces:

$$\Theta_1(x^*, 1) = \Theta_s(x^*, 1), \qquad \frac{\partial \Theta_1}{\partial r}(x^*, 1) = K_s \frac{\partial \Theta_s}{\partial r}(x^*, 1) \tag{4a}$$

$$\Theta_2(x^*, 1+\Delta) = \Theta_s(x^*, 1+\Delta), \qquad \frac{\partial \Theta_2}{\partial r}(x^*, 1+\Delta) = \frac{K_s}{K_f}\frac{\partial \Theta_s}{\partial r}(x^*, 1+\Delta) \tag{4b}$$

The wall temperature and the heat flux at the solid-fluid interfaces, as well as the bulk fluid temperature and the local Nusselt number, have practical significance. They are defined as

$$\Theta_{w1} = \Theta_s(x^*, 1) \tag{5a}$$

$$\Theta_{w2} = \Theta_s(x^*, 1+\Delta) \tag{5b}$$

$$q_1 = \left(\frac{\partial \Theta_1}{\partial r}\right)_w \tag{6a}$$

$$q_2 = K_f(1+\Delta)\left(\frac{\partial \Theta_2}{\partial r}\right)_w \tag{6b}$$

$$\Theta_{b1} = 1 + 8\int_0^{x^*} q_1\, d\xi^* \tag{7a}$$

$$\Theta_{b2} = \Gamma + \frac{8}{1+\Delta}\frac{B}{H}\int_0^{z^*} q_2\, d\zeta^* \tag{7b}$$

$$\mathrm{Nu}_{x1} = 2\,\frac{q_1}{\Theta_{w1} - \Theta_{b1}} \tag{8a}$$

$$\mathrm{Nu}_{x2} = \frac{2}{K_f}\,\frac{B-(1+\Delta)}{1+\Delta}\,\frac{q_2}{\Theta_{w2} - \Theta_{b2}} \tag{8b}$$

By definition equation (6*b*), the heat flux density q_2 is referred to the inner wall surface ($r = 1$) to allow direct comparison with q_1. Equations (5*b*), (6*b*), and (8*b*) hold for both the concurrent and the countercurrent flow case. Equation (7*b*) is written for countercurrent flow heat exchangers. The proper form for the concurrent flow case is obtained by changing the variables z^* and ζ^* with $x^* = L^* - z^*$ and $\xi^* = L^* - \zeta^*$, respectively. Finally, Γ in equation (7*b*) is the ratio of the inlet fluid temperatures T_{02} and T_{01} measured on the thermodynamic Kelvin scale.

The overall rate of entropy production, S, will be used to quantify the heat transfer process according to a second law point of view. Following London and Shah (1983), this quantity is nondimensionalized as

$$\Sigma = \frac{S\,T_{01}}{Q}$$

where Q is the total amount of heat transferred per unit time from stream 2 to stream 1.

The local entropy production rate per unit volume, s, is nondimensionalized and is expressed as follows (de Groot and Mazur, 1962):

$$\sigma = \frac{k_s\, a\, T_{01}}{Q}\,\frac{1}{\Theta^2}\left(\left(\frac{1}{2\,\mathrm{Pe}_1}\frac{\partial \Theta}{\partial x^*}\right)^2 + \left(\frac{\partial \Theta}{\partial r}\right)^2\right) \tag{9}$$

Equation (9) holds for the solid wall. It applies to the fluid regions as well, viscous dissipation in the fluids having been disregarded. The total entropy production rate can be split into three terms Σ_1, Σ_2, and Σ_s, pertaining to the fluid streams and the wall, respectively. One therefore has

$$\Sigma = \Sigma_1 + \Sigma_2 + \Sigma_s \tag{10}$$

The latter term is given as:

$$\Sigma_s = 4\pi\,\mathrm{Pe}_1 \int_1^{1+\Delta}\int_0^{L^*} \sigma_s r\, dr\, dx^* \tag{11}$$

Similar expressions can be written for Σ_1 and Σ_2. However, the following alternative forms have been used here:

$$\Sigma_1 = 4\pi\,\mathrm{Pe}_1 \int_0^{L^*} q_1\left(\frac{1}{\Theta_{b1}} - \frac{1}{\Theta_{w1}}\right) dx^* \tag{12a}$$

$$\Sigma_2 = 4\pi(1+\Delta)\mathrm{Pe}_1 \int_0^{L^*} q_2\left(\frac{1}{\Theta_{w2}} - \frac{1}{\Theta_{b2}}\right) dx^* \tag{12b}$$

These or equivalent expressions are commonly found in the literature (see, e.g., equation (5) from Bejan, 1982), to calculate the entropy production rate in pipe flow heat transfer. Equations (12) are used here for convenience, since Θ_b, Θ_w, and q are known at the end of the computational procedure, while the temperature distributions in the fluids are not. Also, equations (12) allow the numerical results to be checked against the integral entropy balance. This reads

$$\Sigma = \frac{1}{\Theta_{b1}(L^*) - 1}\left(\ln \Theta_{b1}(L^*) + H \ln\left(\Theta_{b2}(L^*)/\Gamma\right)\right) \tag{13}$$

The thermodynamic performance of heat exchangers is usually expressed in terms of the effectiveness, ϵ, and defined as:

$$\epsilon = \frac{Q}{(m\,c_p)_{\min}\,(T_{02} - T_{01})} \tag{14}$$

From equations (13) and (14), the following relations between Σ and ϵ are easily demonstrated:

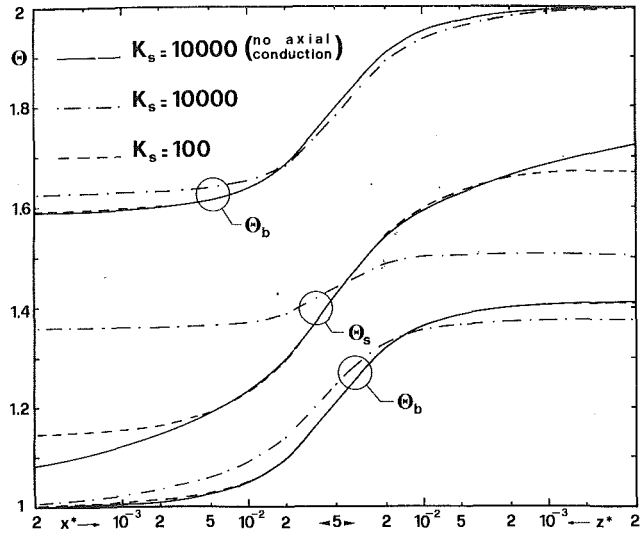

Fig. 2 Axial distributions of bulk fluid and wall (radially averaged) nondimensional temperatures; $H=1$, $Pe_1=500$, $L=100$, $B=6$, $\Delta=0.5$, and $K_f=1$

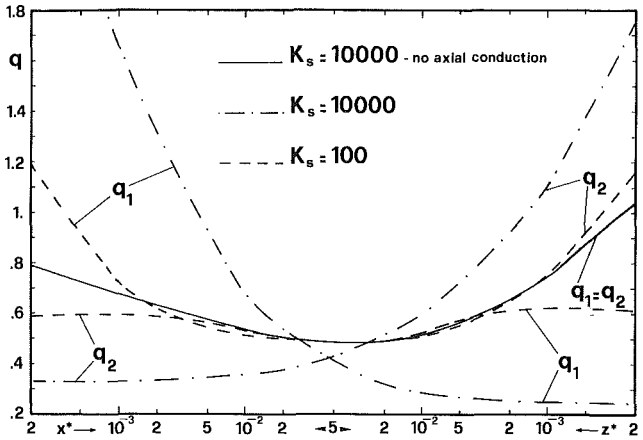

Fig. 3 Axial distributions of the nondimensional heat flux at wall-to-fluid interfaces; $H=1$, $Pe_1=500$, $L=100$, $B=6$, $\Delta=0.5$, and $K_f=1$

$$\frac{\Sigma}{1-1/\Gamma}=\frac{1}{\epsilon}\frac{\Gamma}{(\Gamma-1)^2}\left\{\ln\left[1+\epsilon(\Gamma-1)\right]+H\ln\left[1-\frac{\epsilon}{H}\left(1-\frac{1}{\Gamma}\right)\right]\right\} \quad (15a)$$

for $H>1$, and

$$\frac{\Sigma}{1-1/\Gamma}=\frac{1}{\epsilon}\frac{\Gamma}{(\Gamma-1)^2}\left\{\frac{1}{H}\ln\left[1+\epsilon H(\Gamma-1)\right]+\ln\left[1-\epsilon\left(1-\frac{1}{\Gamma}\right)\right]\right\} \quad (15b)$$

for $H<1$. The quantity $(1-1/\Gamma)$ is used here as a normalization factor for Σ.

4 Procedure and Accuracy

A seminumerical method had been suggested (Barozzi and Pagliarini, 1984, 1985) to deal with conjugated heat transfer in pipe flow. This has been extended to the case of parallel flow heat exchangers. The technique relies upon the application of the superposition principle at the solid–fluid interfaces, and the numerical solution of the energy equation in the wall, by a finite element method. A detailed description of the method having been given elsewhere (Barozzi and Pagliarini, 1985), the procedure will be simply outlined here.

By applying the Duhamel theorem at the solid wall boundaries, one has

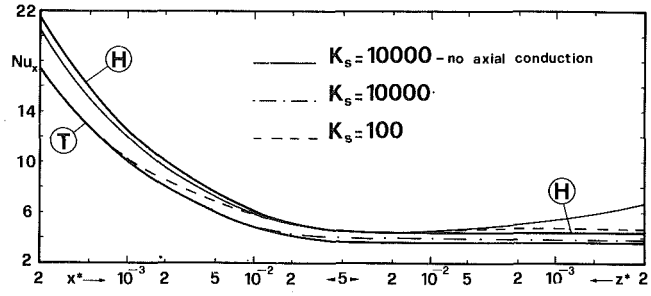

Fig. 4 Axial distributions of the local Nusselt number for inner stream, and reference one-stream data for boundary conditions (H) and (T); $H=1$, $Pe_1=500$, $L=100$, $B=6$, $\Delta=0.5$, and $K_f=1$

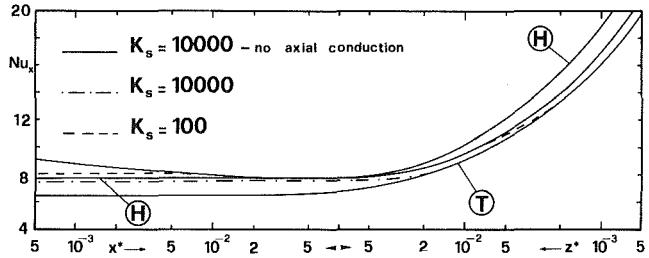

Fig. 5 Axial distributions of the local Nusselt number for outer stream, and reference one-stream data for boundary conditions (H) and (T); $H=1$, $Pe_1=500$, $L=100$, $B=6$, $\Delta=0.5$, and $K_f=1$

$$\Theta_w(x^*)-\Theta_{b1}(x^*)=q_1(0)\frac{2}{\mathrm{Nu}_H(x^*)}+\int_0^{x^*}\frac{2}{\mathrm{Nu}_H(x^*-\xi^*)}\frac{dq_1(\xi^*)}{d\xi^*}\,d\xi^* \quad (16)$$

The expression holds for both streams 1 and 2. In the case of countercurrent flow, however, x^* and ξ^* must be replaced by z^* and ζ^*, respectively, when referring to the outer stream. Nu_H designates the local Nusselt number distribution for a uniformly heated circular (stream 1) or annular (stream 2) duct. Nu_H values are from the literature (Shah and London, 1978). Equation (16) allows the wall-to-fluid temperature differences to be computed for arbitrary distributions of the heat flux.

The computational procedure is iterative. It is initialized with guessed distributions of Θ_b and Nu_x. These complete the set of boundary conditions for equation (2). The energy equation in the wall is solved numerically, by a finite element method. Triangular elements with linear temperature distribution are used in the discretization procedure. From the distribution of Θ_s, updated values of q_1, q_2, Θ_{b1}, and Θ_{b2} are obtained through equations (6) and (7) respectively. Wall-to-fluid temperature differences are then computed by equation (16) and Nu_x distributions obtained from equations (8) to start a new run. The prescribed convergency level was based on the total heat transfer rate, Q, and set equal to 0.001 percent. In all the cases considered, convergence was achieved in less than 14 iterations. Distributions of Nu_x, q, Θ_w, and Θ_b are available at the end of the computational process. The entropy production rates are thus computed by equations (9)–(12). Temperature distributions in the fluid streams are not needed and not computed. However, they can be obtained by superposition, when necessary.

Previous numerical experiments with single-stream problems (Barozzi and Pagliarini, 1984, 1985) showed that the accuracy of Nu_x values is better than 2 percent. Direct comparison with results for the two-stream case is more difficult, since no tabulated data have been found in the open literature. Two checks have been attempted against the available results given in graphic form for the countercurrent case. Omitting axial conduction in the wall, Θ_w and Nu_x distributions have been compared with Nunge and Gill's (1966, Figs. 5 and 7) results.

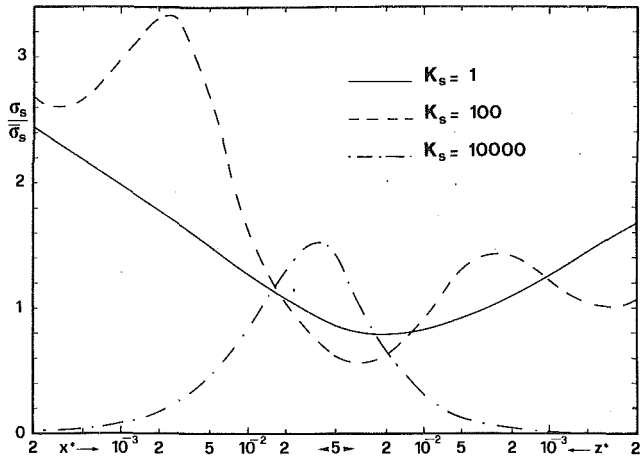

Fig. 6 Axial distributions of local entropy production rate (radially averaged) for the wall; values referred to the mean values of σ_s; $\Gamma = 2$, $H = 1$, $Pe_1 = 500$, $L = 100$, $B = 6$, $\Delta = 0.5$, and $K_f = 1$

Maximum deviations of 6 and 10 percent have been found, respectively. This can be considered acceptable in view of the moderate level of accuracy of the results given by Nunge and Gill (1966), as discussed by Stein (1966b, 1966c). No results being available on account of axial wall conduction in double-pipe heat exchangers, a version of the program has been specifically prepared to provide comparison with the data of Mori et al. (1980) for parallel plate heat exchangers. The agreement with the results shown by Mori et al. (1980, Fig. 10) has been very good.

5 Results

Both the concurrent and countercurrent flow configurations have been investigated. However, only results for the countercurrent case will be presented and discussed in detail.

From the above analysis, the nondimensional groups relevant to the problem are K_s, K_f, B, Δ, L, H, and Pe_1. The absolute temperature ratio Γ also appears in the formulation as far as the problem is considered under a second law point of view. Throughout this analysis, Γ is kept constant at a value of $\Gamma = 2$. It is worth pointing out that, for any value of Γ, Σ can be computed by equations (15) from given values of ϵ and H. Note that the effectiveness concept derives from first law considerations; thus ϵ is independent of Γ. The range covered by the present investigation is as follows: $L = 10$ and 100; $\Delta = 0.5$ and 2; $B = 3$ and 6; $K_s = 1$, 10, 100, 1000, and 10,000; $K_f = 0.1$, 1, and 5; $Pe_1 = 500$, 1000, and 10,000; $H = 0.5$, 1, and 2.

The effect of thermal coupling of the two streams is well illustrated by the distributions of heat flux and temperature at the wall interfaces, as well as the fluid bulk temperature and the Nusselt number for the two streams. Plots of those quantities are presented in Figs. 2, 3, 4, and 5 for a relatively long ($L = 100$), balanced ($H = 1$) heat exchanger. All these quantities are independent of Γ. Data for that single case allow the general trend of the results to be described. Note that in the figures use is made of two separate scales for x^* and $z^* = L^* - x^*$, one running left to right and one running right to left, from the extremities to the middle of the device length.

When overlooking axial heat conduction in the wall, heat transfer results are characterized as follows (Pagliarini and Barozzi, 1984a); (*i*) The temperature of the incoming fluid coincides with the wall temperature at the inlet section; (*ii*) the nondimensional heat flux density is point by point equal on the two sides of the wall, and, typically, its distribution shows a minimum in the central part of the heat transfer region; and (*iii*) for each stream, the distribution of the Nusselt number rapidly decreases near the inlet section of the stream, Nu_x ranging between Nu_T and Nu_H distributions (i.e., single-stream

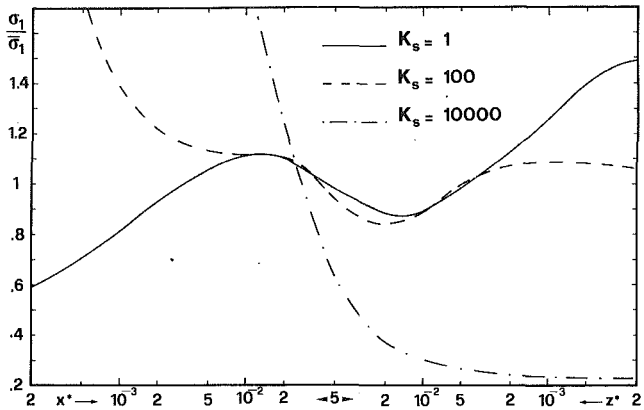

Fig. 7 Axial distributions of local entropy production rate (radially averaged) for the inner stream; values referred to the mean value of σ_1; $\Gamma = 2$, $H = 1$, $Pe_1 = 500$, $L = 100$, $B = 6$, $\Delta = 0.5$, and $K_f = 1$

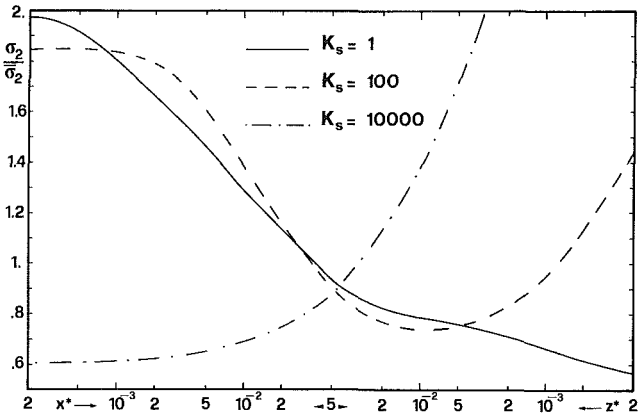

Fig. 8 Axial distributions of local entropy production rate (radially averaged) for the outer stream; values referred to the mean value of σ_2; $\Gamma = 2$, $H = 1$, $Pe_1 = 500$, $L = 100$, $B = 6$, $\Delta = 0.5$, and $K_f = 1$

results for boundary condition (T) and (H), respectively). Nu_x plots take on a minimum, and eventually show a constant value region in the central part of the heat exchanger.

All the above trends are modified in the presence of axial conduction in the wall:

(*i*) Two isothermal areas are created at the wall-to-fluid interfaces, close to the extremities, and the wall temperature does not coincide any further with the inlet fluid temperatures at $x^* = z^* = 0$. The wall-to-fluid temperature difference and the length of the isothermal zones both increase for increase of axial conduction effects. This is well illustrated in Fig. 2 where the effect of the wall conductivity is stressed. It is observed that for increasing K_s, the wall temperature tends to become more uniform, and the outlet temperature of the internal stream, $\Theta_{b1}(x^* = L^*)$ decreases while $\Theta_{b2}(z^* = L^*)$ increases correspondingly. As a consequence, the total heat flux and the effectiveness of the heat exchanger reduce.

(*ii*) Axial wall conduction also uncouples the heat transfer processes on the two sides of the wall. Plots in Fig. 3 still display a general trend similar to the one observed in the absence of axial conduction up to $K_s = 100$: A central zone is found, where the heat flux density is uniform and equal over the two sides of the wall. The situation completely changes for high K_s, the q plots taking on a monotonically decreasing trend from the inlet to the outlet with one single crossing point.

(*iii*) The effect of axial wall conduction on the distributions of the Nusselt number is demonstrated by the coincidence of Nu_x with the corresponding (circular duct or annulus) single-stream solution, case (T), near the inlet section. Farther downstream, both Nu_x and q reach an asymptotic value in the cases shown in Figs. 4 and 5. For low K_s values this may be higher

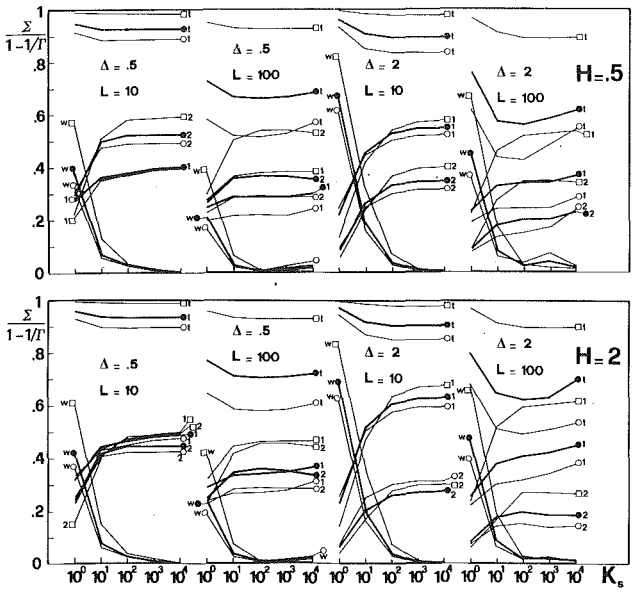

Fig. 9 Normalized nondimensional entropy production rate, as a function of nondimensional thermal conductivity of the wall, K_s; $\Gamma = 2$, $B = 6$, and $K_f = 1$; legend: *w*: in the wall; 1: in the inner stream; 2: in the outer stream; *t*: total value; ○: $Pe_1 = 500$; ●: $Pe_1 = 1000$; □: $Pe_1 = 10{,}000$

than the fully developed one-stream value, case (H), but approximates solution (T) for increasing K_s.

Distributions of the local entropy production rate in the streams and the wall are presented in Figs. 6, 7, and 8 for $\Gamma = 2$. Here, σ has been averaged radially over the section of the region (stream or wall) concerned, and referred to the mean entropy generation rate in the region itself. The results allow some insight to be attained into the irreversible nature of the heat transfer process.

It can be observed first, that distributions of σ in the wall and the streams are quite sensitive to variations in the wall conductivity. For $K_s = 10{,}000$, the local entropy production in the fluids is maximum at the inlet sections, and decreases monotonically downstream. For reducing K_s, the plots of σ_1 and σ_2 take on a less regular trend, eventually presenting intermediate maxima and minima, and the values decrease progressively at the inlet, while increasing in the outlet regions. The local entropy generation rate in the fluids is related to q, Θ_w, and Θ_b as from equations (12). The above behavior can therefore be interpreted in the light of Figs. 2 and 3 from which it is possible to deduce that the maxima in σ_1 and σ_2 correspond to axial positions where either the heat flux density or the wall-to-fluid temperature difference are relatively high.

Distributions of σ_s indicate that the effect of the radial thermal resistence of the wall is dominant when K_s is low. Entropy generation is a minimum in the central region and a maximum at the extremities for $K_s = 1$. Such a trend is typical in the absence of axial conduction (Pagliarini and Barozzi, 1984b). The situation is completely reversed when K_s is very high. For $K_s = 10{,}000$ a maximum is found in the middle of the wall length, where the axial temperature gradient is higher. The entropy production falls to zero at the wall extremities, where the wall is isothermal. Case $K_s = 100$ represents an intermediate situation where the entropy production rates due to the axial and radial conduction tend to be in balance. All the above trends are not substantially modified by variations of H over the range covered by this analysis.

The role of the wall conductivity, K_s, has been particularly stressed by the results. However, the significance of the observations is more general, results for low K_s values being representative of situations where the effect of heat conduction along the wall is moderate, and vice versa.

Table 1 Effectiveness of countercurrent heat exchangers, $B = 6$ and $K_f = 1$

Δ=0.5	L=10	|	ε						
Pe_1 ⇓	H ⇓	K_{opt} ⇓	K_s= 1	10	100	1000	10000	10000*	K_{opt}
500	0.5	83	.115	.155	.157	.153	.153	.163	.157
	1	125	.063	.088	.090	.087	.087	.094	.089
	2	167	.069	.100	.102	.099	.098	.107	.101
1000	0.5	167	.067	.095	.098	.095	.095	.101	.097
	1	250	.037	.055	.056	.055	.054	.058	.056
	2	333	.040	.062	.064	.062	.062	.067	.063
10000	0.5	1667	.010	.019	.020	.020	.020	.021	.020
	1	2500	.005	.011	.012	.012	.012	.012	.012
	2	3333	.006	.012	.014	.014	.013	.014	.013
Δ=0.5	L=100	|	ε						
Pe_1 ⇓	H ⇓	K_{opt} ⇓	K_s= 1	10	100	1000	10000	10000*	K_{opt}
500	0.5	83	.572	.655	.662	.647	.597	.666	.662
	1	125	.340	.403	.409	.401	.376	.412	.409
	2	167	.378	.457	.465	.457	.431	.468	.464
1000	0.5	167	.378	.456	.464	.459	.438	.467	.464
	1	250	.214	.266	.272	.268	.257	.273	.271
	2	333	.234	.298	.305	.302	.289	.307	.304
10000	0.5	1667	.067	.096	.100	.100	.098	.101	.100
	1	2500	.037	.055	.058	.058	.056	.058	.057
	2	3333	.040	.063	.066	.066	.065	.067	.066
Δ=2	L=10	|	ε						
Pe_1 ⇓	H ⇓	K_{opt} ⇓	K_s= 1	10	100	1000	10000	10000*	K_{opt}
500	0.5	83	.092	.207	.227	.227	.227	.249	.227
	1	125	.048	.115	.128	.128	.128	.141	.128
	2	167	.050	.125	.142	.142	.142	.156	.142
1000	0.5	167	.050	.128	.146	.146	.146	.159	.146
	1	250	.026	.070	.082	.082	.082	.090	.082
	2	333	.027	.077	.091	.091	.091	.100	.091
10000	0.5	1667	.006	.023	.032	.033	.033	.035	.033
	1	2500	.003	.013	.018	.018	.018	.020	.018
	2	3333	.003	.014	.020	.021	.021	.022	.021
Δ=2	L=100	|	ε						
Pe_1 ⇓	H ⇓	K_{opt} ⇓	K_s= 1	10	100	1000	10000	10000*	K_{opt}
500	0.5	83	.525	.765	.781	.702	.628	.808	.783
	1	125	.305	.488	.511	.475	.437	.525	.509
	2	167	.330	.552	.584	.557	.524	.597	.582
1000	0.5	167	.335	.570	.605	.571	.529	.620	.602
	1	250	.184	.337	.364	.351	.331	.373	.362
	2	333	.194	.372	.406	.395	.376	.415	.403
10000	0.5	1667	.050	.130	.155	.155	.149	.159	.153
	1	2500	.026	.072	.087	.087	.084	.090	.086
	2	3333	.027	.078	.097	.097	.093	.100	.095

*: no axial conduction.

The number of the relevant nondimensional quantities being so large, their influence on the thermal behavior of the device cannot be considered in terms of the local entropy production rate. The effect of each parameter is more conveniently estimated by resorting to the total entropy production rate Σ, or the heat exchanger effectiveness, ϵ.

The nondimensional entropy generation rate Σ, and its components, Σ_1, Σ_2, and Σ_s, are shown in Fig. 9. Values of ϵ for changing Δ, L, Pe_1, H, and K_s are presented in Table 1. Values of effectiveness corresponding to the optimum value of the wall conductivity, K_{opt}, have also been computed by the same procedure for all the cases considered, and results listed in Table 1. K_{opt} is defined according to Chowdhury and Sarangi (1983, equation (11)) and is a function of Pe_1 and H. Finally, results in the absence of axial wall conduction are given for the sake of comparison. These are for $K_s = 10{,}000$.

It is pointed out that the effectiveness of the heat exchanger

no longer increases monotonically with K_s, as it would do in the absence of axial conduction in the wall. Instead, for any choice of Pe_1 and H, a minimum can be identified for Σ, and a corresponding maximum for ϵ at an intermediate value of K_s.

For low K_s, most of the entropy production is concentrated in the wall, due to the effect of radial heat conduction. In a short heat exchanger ($L = 10$), while increasing K_s the contribution of the wall decreases monotonically, the wall approaches an isothermal condition, Σ_s goes to zero, and Σ_1, Σ_2 approach a constant value independent of K_s. In a long device ($L = 100$), however, the increase in the entropy production due to axial conduction in the wall competes with the reduction in the radial contribution for increasing K_s. Thus, a minimum is observed in Σ_s for K_s of order 100. This is found to be representative of a condition of maximum effectiveness and minimum total entropy production. Neither a situation of the wall being isothermal nor Σ having a constant value is usually found in a long heat exchanger for K_s up to 10,000.

From data in Table 1, it is observed that ϵ is a minimum for $H = 1$ irrespective of the choice of other nondimensional quantities. When analyzing the results in terms of the entropy production rate, however, it is found that Σ_1 decreases and Σ_2 increases systematically for increasing H from 0.5 to 2. Overall, the total entropy production rate, Σ, is practically insensitive to variations of H for short heat exchangers ($L = 10$). Variations of Σ with H are less than 1 percent in those cases. The same holds true for long heat exchangers ($L = 100$), provided that $Pe_1 \geq 1000$. For lower values of Pe_1 and $L = 100$, however, changing H from 0.5 to 2 produces a definite increase in Σ (from 5 to 20 percent). From a second law point of view, then, operating conditions corresponding to values of H higher than one should be avoided in high-performance devices.

Increasing Pe_1 always reduces the negative influence of longitudinal heat conduction, but also causes deterioration in the overall performance of the device.

Long heat exchangers are found to be more sensitive to the variation of the wall conductivity than short devices. This finding looks contradictory since the effect of axial heat conduction is expected to be more pronounced when L is low. However, it must be emphasized that short heat exchangers are basically characterized by a very high rate of entropy production. Any additional contribution to it is thus of moderate importance in relative terms.

Table 1 indicates that values of ϵ are higher for $\Delta = 2$ than for $\Delta = 0.5$. When interpreting such a behavior, it should be born in mind that increasing Δ at equal Pe_1 and H produces a relative increase of the mean fluid velocity of the external stream, the flow rate remaining unchanged. The effectiveness of the heat exchanger increases as a consequence. The same holds true for reducing B as can be seen by comparing data in Table 1 with results given in Table 2. The percentage reduction in effectiveness due to axial wall conduction definitely increases for increasing wall thickness, while it is little influenced by variations in the pipe diameter ratio. It is worth pointing out, however, that the entropy production inherent in the fluid-dynamic process is not taken into account in this analysis. That term increases for an increase in the mean velocity of flow.

All other quantities being fixed, the effectiveness also increases monotonically for increasing K_f, as from Table 3. That behavior should be ascribed to the reduction of the convective thermal resistence of the external stream that occurs for increasing K_f.

The criterion given by Chowdhury and Sarangi (1983) to predict the optimum value of the wall conductivity was based on some crude approximation. Nonetheless it is found to agree very favorably with the results of the present analysis. From data in Table 1, the values of ϵ obtained for $K_s = K_{opt}$ systematically approach the maximum. The criterion tends to become slightly less accurate and reliable when the effectiveness is very low.

Table 2 Effectiveness of countercurrent heat exchangers, $B = 3$ and $K_f = 1$

Δ=0.5	L=100				ϵ			
Pe_1 ⇓	H ⇓	K_{opt} ⇓	K_s= 1	10	100	1000	10000	K_{opt}
500	0.5	83	.676	.792	.802	.775	.682	.802
	1	125	.414	.511	.521	.510	.466	.521
	2	167	.460	580	.593	.585	.549	.593
1000	0.5	167	.472	.601	.616	.605	.561	.615
	1	250	.270	.359	.370	.366	.346	.369
	2	333	.292	.398	.412	.408	.391	.411
10000	0.5	1667	.088	.147	.158	.158	.154	.157
	1	2500	.047	.082	.089	.089	.087	.089
	2	3333	.050	.091	.099	.099	.097	.098

Table 3 Effectiveness of countercurrent heat exchangers for different values of K_f; $B = 6$ and $Pe_1 = 500$

Δ=0.5	L=100				ϵ		
Pe_1 ⇓	H ⇓	K_s= 1	10	100	1000	10000	
500	0.5	.192	.200	.201	.199	.195	K_f=0.1
	1	.113	.119	.120	.119	.116	
	2	134	.142	.143	.141	.137	
500	0.5	.572	.655	.662	.647	.597	K_f=1
	1	.340	.403	.409	.401	.376	
	2	.378	.457	.465	.457	.431	
500	0.5	.725	.857	.867	.833	.707	K_f=5
	1	.451	.568	.581	.568	.508	
	2	.501	.642	.659	.652	.614	

As far as concurrent flow heat exchangers are concerned, computations have been restricted to the case of balanced flow, $H = 1$. Results have been presented elsewhere (Pagliarini and Barozzi, 1984a). They indicate that the effects of axial conduction in the wall are minor, with respect to the corresponding counterflow cases. Local quantities, such as the wall and the fluid temperatures, are actually only moderately influenced. The overall effectiveness of the device is totally unaffected by the presence of heat conduction along the wall.

6 Concluding Remarks

Local and overall effects of thermal coupling in laminar counterflow double-pipe heat exchangers have been considered on account of axial heat conduction in the wall separating the streams. The range covered by this analysis has been deliberately limited, in view of the considerable number of geometric, thermal, and flow parameters involved in the problem. A few conclusions of a general validity are however permitted.

It is observed first that conduction along the thermally active wall may have a definite effect upon the distributions of the most important thermal quantities, such as the wall temperature, the heat flux, the bulk fluid temperature, and the Nusselt number. The extent of such an influence depends however on a number of geometric, thermal, and flow variables, forming a set of seven independent nondimensional groups. Therefore, local effects of thermal coupling and axial wall conduction have been mainly concerned with the effect of the wall conductivity parameter, K_s. The presence of axial wall conduction is revealed by the wall temperature tending to become longitudinally uniform. The effect starts at the wall extremities, where two isothermal regions are observed, however low the value of K_s is. These lengthen progressively for increasing K_s, finally covering the entire heat transfer section as the wall conductivity tends to infinity. Correspondingly, the two streams become thermally uncoupled in the sense that each current approaches the thermal behavior typical of a single-stream

case, subject to the boundary condition of uniform wall temperature. In the limit of high K_s values, then, single-stream Nu_T correlations apply.

The thermodynamic behavior of the equipment can either be considered under a traditional first law point of view, or expressed in terms of the entropy production rate following a second law approach. It is observed that the two methods lead to perfectly equivalent results as far as the overall performance of the equipment is concerned. In fact, the heat exchanger effectiveness, ϵ, and the total entropy production rate, Σ, are related in a very simple way. The second law approach, however, gives a deeper insight into the irreversible nature of the heat transfer process, and therefore offers a more reliable design tool.

The performance of countercurrent heat exchangers has been investigated, as affected by the operative conditions, the thermal properties of the wall and the fluids, and the geometry of the equipment.

Results indicate that increasing the Peclet number, e.g., by increasing the flow rate, while leaving constant the heat capacity ratio, H, always produces a reduction in the heat exchanger effectiveness. On the other hand, for increasing H from 0.5 to 2, a minimum is observed in ϵ, for balanced heat exchangers. In terms of the entropy production rate, however, it is found that the performance of the device is influenced negatively by high values of H. That conclusion is of chief concern for devices whose effectiveness is basically very high, as is the case of a long heat exchanger. Increasing the fluid conductivity ratio, K_f, has a strong and positive effect on effectiveness. Changing the wall thickness or the diameter of the outer duct, i.e., changing Δ or B, all other conditions being unchanged, corresponds to considering a quite different physical situation. The results must therefore be interpreted with some care. In any case they indicate a reduction of the performance in the case of a long and very efficient heat exchanger, both for decreasing Δ and increasing B. Also note that relatively high values for the wall thickness have been used in the present analysis to emphasize the influence of axial wall conduction on local quantities. Results are however of practical significance, since they offer clear directions for conduction-penalty minimization.

The effects of the wall conductivity have been particularly stressed in the analysis. It is found that a region of minimum entropy production always exists in the range of variability considered for K_s. The need for optimizing the wall conductivity becomes the more stringent as the equipment effectiveness increases. In this connection, the simple criterion suggested by Chowdhury and Sarangi (1983) has been proved to give reliable indications over a wide range of operative conditions. Thus, the analysis indicates that a proper choice of the wall material is needed for the thermal performance optimization of laminar flow double pipe heat exchangers. To exemplify, if heat is exchanged between two countercurrent water streams separated by a copper wall ($K_s \approx 600$), axial conduction in the wall is expected to produce a small, but definite, decrease in the effectiveness. The optimum value could be attained using a steel wall, characterized by a K_s value of about 100. If, instead, a glass wall is used, the order of magnitude of K_s drops to 1, and the effectiveness decreases sharply due to the introduction of a high radial thermal resistance. The effects of axial wall conduction are more pronounced when gaseous fluids are considered. If, indeed, two air streams and a cooper wall are used, K_s becomes higher than 10,000. A reduction of a few percentage units in the device effectiveness can result, with respect to the optimum value. Once again, the latter can be approximated using a steel wall ($K_s \approx 1000$).

As far as concurrent flow heat exchangers are concerned, previous work (Pagliarini and Barozzi, 1984a) has demonstrated that the effects of wall conductivity are minor.

This conclusion, however, is restricted to the case of balanced heat exchangers, and further analyses are needed to generalize it.

Acknowledgments

The authors acknowledge the useful remarks of the Referees, and the help of Dr. M. W. Collins, The City University, London, during the revision of the paper. The research has been supported by M.P.I., and C.N.R. under grant No. 89.03276.07.

References

Barozzi, G. S., and Pagliarini, G., 1984, "Conjugated Heat Transfer in a Circular Duct With Uniform and Non-uniform Wall Thickness," *Heat and Technology*, Vol. 2, pp. 72–91.

Barozzi, G. S., and Pagliarini, G., 1985, "A Method to Solve Conjugate Heat Transfer Problems: the Case of Fully Developed Laminar Flow in a Pipe," ASME JOURNAL OF HEAT TRANSFER, Vol. 107, pp. 77–83.

Barron, R. F., and Yeh, S. L., 1976, "Longitudinal Conduction in Three-Fluid Heat Exchangers," ASME Paper No. 76-WA/HT-9.

Bejan, A., 1977, "The Concept of Irreveribility in Heat Exchanger Design: Counterflow Heat Exchangers for Gas-to-Gas Applications," ASME JOURNAL OF HEAT TRANSFER, Vol. 99, pp. 374–380.

Bejan, A., 1982, "Second-Law Analysis in Heat Transfer and Thermal Design," in: *Advances in Heat Transfer*, Vol. 15, T. F. Irvine and J. P. Hartnett, eds., Academic Press, New York, pp. 1–58.

Bentwich, M., 1970, "Concurrent and Countercurrent Parabolic Flow Heat Exchangers," *Israel Journal Technology*, Vol. 8, pp. 197–207.

Bentwich, M., 1973, "Multistream Countercurrent Heat Exchangers," ASME JOURNAL OF HEAT TRANSFER, Vol. 95, pp. 458–463.

Blanco, J. A., and Gill, W. N., 1967, "Analysis of Multistream Turbulent Forced Convection Systems," *Chemical Engineering Progress Symposium Series 77*, Vol. 63, pp. 66–79.

Blanco, J. A., Gill, W. N., and Nunge, R. J., 1968, "Computational Procedures for Recent Analyses of Counterflow Heat Exchangers," *AIChE Journal*, Vol. 14, pp. 505–507.

Chiou, J. P., 1983, "Thermal Performance Deterioration in Crossflow Heat Exchanger Due to Longitudinal Heat Conduction and Nonuniform Inlet Fluid Temperature Distribution," *Proceedings ASME-JSME Thermal Engineering Joint Conference*, Honolulu, HI, Vol. 2, pp. 451–458.

Chowdhury, K., and Sarangi, S., 1983, "A Second Law Analysis of the Concentric Tube Heat Exchanger: Optimization of Wall Conductivity," *International Journal of Heat and Mass Transfer*, Vol. 26, pp. 783–786.

Ciampi, M., and Tuoni, G., 1979, "Considerazioni Termodinamiche sugli Scambiatori di Calore (On the Thermodynamic Behavior of Heat Exchangers)," *La Termotecnica*, Vol. 33, pp. 186–197.

Cotta, R. M., and Ozisik, M. N., 1986, "Thermally Developing Concurrent-Flow Circular Double-Pipe Heat Exchanger Analysis," *Proceedings Eighth Heat Transfer Conference*, Vol. 6, San Francisco, pp. 2805–2810.

de Groot, S. R., and Mazur, P., 1962, *Non-Equilibrium Thermodynamics*, North Holland, Amsterdam, Netherlands.

Gill, W. N., Porta, E. W., and Nunge, R. J., 1968, "Heat Transfer in the Thermal Entrance Region of Concurrent Flow Heat Exchangers With Fully Developed Laminar Flow," *International Journal of Heat and Mass Transfer*, Vol. 11, pp. 1408–1412.

Golem, P. J., and Brzustowski, T. A., 1976, "Second-Law Analysis of Energy Processes, Part II: the Performance of Simple Heat Exchangers," *Trans. Can. Soc. Mech. Engrs.*, Vol. 4, pp. 219–226.

Kakac, S., Bergles, A. E., and Mayinger, F., 1981, *Heat Exchangers, Thermal-Hydraulic Fundamentals and Design*, Springer-Verlag, Berlin, Germany.

Kays, W. M., and London, A. L., 1984, *Compact Heat Exchangers*, 3rd ed., McGraw-Hill, New York.

Kroeger, P. G., 1966, "Performance Deterioration in High Effectiveness Heat Exchangers Due to Axial Heat Conduction Effects," *Advances Cryogenic Engineering*, Vol. 12, pp. 364–372.

Lin, T. F., and Tsay, Y. L., 1986, "Thermal Interactions in Countercurrent-Flow Double-Pipe Heat Exchangers," *Proceedings Eighth Heat Transfer Conference*, Vol. 6, San Francisco, pp. 2811–2816.

London, A. L. and Shah, R. K., 1983, "Costs of Irreversibilities in Heat Transfer Exchanger Design," *Heat Transfer Engineering*, Vol. 4, pp. 59–73.

Mikhailov, M. D., 1972, "General Solutions of the Heat Equations in Finite Regions," *International Journal of Engineering Science*, Vol. 10, pp. 577–591.

Mikhailov, M. D., 1973a, "General Solutions of the Diffusion Equations Coupled at Boundary Conditions," *International Journal of Heat and Mass Transfer*, Vol. 16, pp. 2155–2164.

Mikhailov, M. D., 1973b, "General Solutions of the Coupled Diffusion Equations," *International Journal of Engineering Science*, Vol. 11, pp 235–241.

Mikhailov, M. D., 1983, "Mathematical Modelling of Heat Transfer in Single Duct and Double Pipe Exchangers," in: *Low Reynolds Number Flow Heat Exchangers*, S. Kakac, R. K. Shah, and A. E. Bergles, eds., Hemisphere Publ. Corp., Washington, DC.

Mikhailov, M. D., and Shishedjiev, B. K., 1976, "Coupled at Boundary Mass or Heat Transfer in Entrance Concurrent Flow," *International Journal of Heat and Mass Transfer*, Vol. 19, pp. 553–557.

Mori, S., Kataya, M., and Tanimoto, A., 1980, "Performance of Counterflow, Parallel Plate Heat Exchangers Under Laminar Flow Conditions," *Heat Transfer Engineering*, Vol. 2, pp. 28–38.

Nunge, R. J., and Gill, W. N., 1965, "Analysis of Heat or Mass Transfer in Some Countercurrent Flows," *International Journal of Heat and Mass Transfer*, Vol. 8, pp. 873–886.

Nunge, R. J., and Gill, W. N., 1966, "An Analytical Study of Laminar Counterflow Double-Pipe Heat Exchangers," *AIChE Journal*, Vol. 12, pp. 279–286.

Nunge, R. J., Porta, E. W., and Gill, W. N., 1967, "Axial Conduction in the Fluid Streams of Multistream Heat Exchangers," *Chemical Engineering Progress Symposium Series*, Series 77, Vol. 63, pp. 80–91.

Pagliarini, G., and Barozzi, G. S., 1984a, "Effetti di Accoppiamento Termico negli Scambiatori Tubo in Tubo a Correnti Laminari (Thermal Coupling in Laminar Double Stream Heat Exchangers)," *Proceedings Second National Conference on Heat Transfer*, Bologna, Italy, pp. 103–113.

Pagliarini, G., and Barozzi, G. S., 1984b, "Produzione di Entropia per Conduzione Termica nella Parete di Scambiatori di Calore a Correnti Contrapposte Bilanciate (Entropy Generation Due to Thermal Conduction Along the Wall of Balanced Counterflow Heat Exchangers)," *Proceedings 39th A.T.I. National Conference*, L'Aquila, Italy, Vol. I, pp. 191–200.

Pagliarini, G., and Barozzi, G. S., 1985, "Ulteriori Considerazioni sulla Produzione di Entropia in Scambiatori di Calore a Correnti Laminari Contrapposte (Further Considerations on Entropy Production in Laminar Countercurrent Heat Exchangers)," *Proceedings Third National Conference on Heat Transfer*, Palermo, Italy, pp. 164–176.

Papoutsakis, E., and Ramkrishna, D., 1981, "Conjugated Graetz Problems," *Chemical Engineering Science*, Vol. 36, pp. 1381–1391, 1393–1399.

Seban, R. A., Hsieh, T. C., and Greif, R., 1972, "Laminar Counterflow Exchangers: an Approximate Account of Wall Resistance and Variable Heat Transfer Coefficients," ASME JOURNAL OF HEAT TRANSFER, Vol. 94, pp. 391–396.

Shah, R. K., and London, A. L., 1978, *Laminar Flow Forced Convection in Ducts*, Academic Press, New York.

Spalding, D. B., 1984, *Heat Exchanger Design Handbook*, Hemisphere, Washington, DC.

Stein, R. P., 1964, "The Graetz Problem in Concurrent-Flow Double-Pipe, Heat Exchangers," ANL Rept. 5889, Argonne National Lab.

Stein, R. P., 1965a, "The Graetz Problem in Concurrent Flow Double Pipe Heat Exchangers," *Chemical Engineering Progress Symposium Series 59*, Vol. 61, pp. 76–87.

Stein, R. P., 1965b, "Heat Transfer Coefficients in Liquid Metal Concurrent Flow Double Pipe Heat Exchangers," *Chemical Engineering Progress Symposium Series 59*, Vol. 61, pp. 64–75.

Stein, R. P., 1966a, "Liquid Metal Heat Transfer," in: *Advances in Heat Transfer*, Vol. 3, T. F. Irvine and J. P. Hartnett, eds., Academic Press, New York.

Stein, R. P., 1966b, "Computational Procedures for Recent Analyses of Counterflow Heat Exchangers," *AIChE Journal*, Vol. 12, pp. 1216–1219.

Stein, R. P., 1966c, "Mathematical and Practical Aspects of Heat Transfer in Double Pipe Heat Exchangers," *Proceedings Third International Heat Transfer Conference*, AIChE, New York, Vol. 1, pp. 139–148.